INTERIM REPORT

Large-Scale Laboratory Experiments of Incipient Motion, Transport, and Fate of Underwater Munitions under Waves, Currents, and Combined-Flows

SERDP Project MR-2410

DECEMBER 2015

Marcelo Garcia
Blake Landry
University of Illinois at Urbana-Champaign

SERDP
DOD ▪ EPA ▪ DOE

REPORT DOCUMENTATION PAGE

Form Approved
OMB No. 0704-0188

1. REPORT DATE *(DD-MM-YYYY)*	**2. REPORT TYPE**	**3. DATES COVERED** *(From - To)*
11-30-2015	Interim Report	May 2015-November 30, 2015

4. TITLE AND SUBTITLE

Large-Scale Laboratory Experiments of Incipient Motion, Transport, and Fate of Underwater Munitions under Waves, Currents, and Combined-Flows

5a. CONTRACT NUMBER
W912HQ-14-C-0032

5b. GRANT NUMBER

5c. PROGRAM ELEMENT NUMBER

6. AUTHOR(S)

Dr. Marcelo H. Garcia
Dr. Blake J. Landry

5d. PROJECT NUMBER
MR-2410

5e. TASK NUMBER

5f. WORK UNIT NUMBER

7. PERFORMING ORGANIZATION NAME(S) AND ADDRESS(ES)

University of Illinois at Urbana-Champaign
205 North Mathews Avenue
Urbana, IL 61801

8. PERFORMING ORGANIZATION REPORT NUMBER

9. SPONSORING / MONITORING AGENCY NAME(S) AND ADDRESS(ES)
Strategic Environmental Research and Development Program (SERDP)
4800 Mark Center Drive
Suite 17D08
Alexandria VA 22350-3600

10. SPONSOR/MONITOR'S ACRONYM(S)
SERDP

11. SPONSOR/MONITOR'S REPORT NUMBER(S)

12. DISTRIBUTION / AVAILABILITY STATEMENT

Approved for public release; distribution is unlimited.

13. SUPPLEMENTARY NOTES
N/A

14. ABSTRACT

We seek to quantify the incipient motion, transport and fate of underwater munitions in coastal environments comprised of mobile beds and/or hard bottoms (e.g., sandy and gravel/rock) under a range of relevant hydrodynamic conditions (e.g., waves, currents, combined flows). The existing underwater phenomenology of munitions expects mobility to be maximized when munitions are proud (i.e., unburied). It has been suggested that the degree of mobility may be orders of magnitude larger when munitions are transported over a hard gravel-like substrate where there is little or no sediment cover (e.g., such as on coral reefs) versus a sandy or muddy bottom. However, there is a dearth of direct observations made under a wide range of controlled hydrodynamics conditions representative of waves and currents. Through an extensive set of detailed large-scale laboratory experiments we plan to develop a complete picture of the phenomena involved in the entrainment, transport, and fate of underwater munitions.

15. SUBJECT TERMS
Unexploded Ordnance, UXO, Underwater Munitions, Incipient Motion, Transport, Fate, Phenomenology, Hydrodynamic Forcing, Vortex Lattice UXO Mobility Model.

16. SECURITY CLASSIFICATION OF:			**17. LIMITATION OF ABSTRACT**	**18. NUMBER OF PAGES**	**19a. NAME OF RESPONSIBLE PERSON**
a. REPORT	**b. ABSTRACT**	**c. THIS PAGE**			Dr. Marcelo Garcia
U	U	U	SAR	36	**19b. TELEPHONE NUMBER** *(include area code)* 217-244-4484

Table of Contents

List of Tables

List of Figures

List of Acronyms

GUI	Graphical User Interface
IHFF	Illinois Hyporheic Flow Facility
IP	Internet Protocol
LOWST	Large Oscillatory Water-Sediment Tunnel (LOWST)
MP	Megapixels
NRL-Stennis	Naval Research Laboratory; Stennis Space Center; Stennis, Mississippi
PIV	Particle Image Velocimetry
PVC	Polyvinyl Chloride
SERDP	Strategic Environmental Research and Development Program
SfM	Structure from Motion
SOT	Small Oscillatory Flume
STF	Small Tilting Flume
UIUC	University of Illinois at Urbana-Champaign
UXO	Unexploded Ordnance
VTCHL	Ven Te Chow Hydrosystems Lab
WHOI	Woods Hole Oceanographic Institution Flume (named after the original location from which the Hydrosystems Lab procured the flume)

Keywords

Initiation of Motion of Munitions, Motion Tracking, Munition Migration, Oscillatory Flow, Particle Image Velocimetry, Physical Laboratory Experiments, Unidirectional Flow

Acknowledgements

We would like to express gratitude to the research team for their dedication and continuous energy in helping to move the project forward which includes the follows researchers:

- Alejandro Vitale, PhD (visiting researcher from Argentina)
- Carlo Zuniga Zamalloa, PhD (postdoctoral researcher)
- Heng Wu, MS (PhD student)
- Stephen Gates (hourly undergraduate student)
- Sarah Wenzel (hourly undergraduate student)
- Nils Oberg, BS (research programmer)
- Andrew Waratuke, MS (research engineer)
- Hannah Morch (hourly undergraduate student)
- Nick Moller (MS student)

Also, we you like to thank the Dr. Joe Calantoni at NRL-Stennis for providing surrogate munitions for our CEE Machine Shop to duplicate for laboratory testing.

1. Abstract

Our research project responds directly to MRSON-14-01 with an emphasis on the need to improve our understanding of the phenomenology of entrainment, transport and fate of underwater munitions. A recent white paper (SERDP 2010, p.4) identified several knowledge gaps in the predictive skill of munitions mobility models. Our proposal is aligned to address these gaps in environments with active sandy beds and hard bottom substrates. Ultimately, the fundamental work performed under our proposal will provide a critical data set for the development of new and improvement of existing field scale models for the mobility of munitions (such as the Vortex Lattice UXO Mobility Model) that are difficult or practically impossible to obtain with existing field measurements.

Work presented herein provides physical laboratory results for initiation of motion and transport of various surrogate munitions over two hard substrates having different roughness (smooth PVC versus pitted steel) in unidirectional flow. In addition, based on flows resulting in initiation of motion, particle image velocimetry measurements were conducted in both unidirectional and oscillatory flows to resolve the flow structure and estimate drag forces to ultimately help develop relationships to predict initiation and transport of munitions. To better track the munitions after initiation and resolve the six-degrees of freedom, optical tracking techniques were developed, deployed, and honed for use in tracking munitions during the main experimental year of the project, year two.

2. Objective

We seek to quantify the incipient motion, transport and fate of underwater munitions in coastal environments comprised of mobile beds and/or hard bottoms (e.g., sandy and gravel/rock) under a range of relevant hydrodynamic conditions (e.g., waves, currents, combined flows). The existing underwater phenomenology of munitions expects mobility to be maximized when munitions are proud (i.e., unburied). It has been suggested that the degree of mobility may be orders of magnitude larger when munitions are transported over a hard gravel-like substrate where there is little or no sediment cover (e.g., such as on coral reefs) versus a sandy or muddy bottom. However, there is a dearth of direct observations made under a wide range of controlled hydrodynamics conditions representative of waves and currents. Through an extensive set of detailed large-scale laboratory experiments we plan to develop a complete picture of the phenomena involved in the entrainment, transport, and fate of underwater munitions. These laboratory experiments will allow for detailed measurements over a controlled range of conditions (e.g., hydrodynamic forcing, turbulence characteristics, sediment bed composition, and properties of munitions) which are not practically possible to achieve in field experiments and cannot be completely simulated with numerical models due to the high Reynolds number and wide-range of bottom roughness observed under field conditions. We seek to aggregate our previous experience on scour and burial of mines with the results from the proposed physical experiments to enhance existing predictive models and advance towards the development of a new *Lagrangian transport/fate model*. The new model will be based on our experience with gravel/sand transport and will account for boundary-layer hydrodynamics, bottom roughness, and munitions characteristics under oscillatory-flow and unidirectional current conditions representative of those observed in coastal environments.

3. Technical Approach

In this study we plan to observe the incipient motion and transport of unexploded ordnance (UXO) through large-scale physical laboratory investigations utilizing two facilities in the Ven Te Chow Hydrosystems Laboratory (VTCHL) at the University of Illinois at Urbana-Champaign (UIUC). Combined oscillating flows with superimposed unidirectional currents are achieved in the following facilities: (1) water tunnel and (2) wave flume, each capable of achieving peak velocities of 2 m/s. We will implement various laboratory techniques (optical, electronic, and acoustic) to provide data on incipient motion, trajectory and rotation of the munitions, hydrodynamic conditions, and sediment transport characteristics. The processed laboratory results will be put into production to improve existing predictive models and advance towards a new Lagrangian transport/fate model.

The first year of our SERDP project was dedicated to preparing both large-scale facilities, i.e., Large Oscillatory Water Sediment Tunnel (LOWST) and Large Wave Current Flume (LWCF) per our SERDP proposal. Several supplementary tasks were performed while the large-scale facilities were being prepared. Initiation of motion experiments with unidirectional flow were performed in several smaller laboratory facilities. Detailed measurements of flow structure using particle image velocimetry with unidirectional and oscillatory flows were conducted to better understand munitions migration. Object tracking techniques such as Structure from Motion (SfM) and motion reconstruction from feature tracking were explored, developed, and honed to enable resolution of munition trajectories during the main set of experiments the second year of our SERDP project. The following subsections detail the technical approaches used while conducting the laboratory experiments (Section 3.1) and developing the motion capture techniques (Section 3.2).

3.1 Laboratory Experiments

3.1.1 Initiation of Motion in Unidirectional Flow

Experimental Facilities

Initiation of motion experiments were conducted in two unidirectional flow facilities in the Ven Te Chow Hydrosystems Laboratory: the WHOI flume and the Small Tilting Flume (STF).

Description of WHOI:

The WHOI flume is a 17.3 m long, 0.6 m wide, and 0.3 m deep fiberglass flume with Plexiglas windows (see Figure 1). The flume has a smooth polyvinyl chloride (PVC) false bottom. Hydraulic pistons allow for adjustment of the bed slope, with the fulcrum located near the downstream end of the flume. A small tank at the downstream end of the flume acts as a reservoir and establishes tail-water conditions. Water is recirculated in the flume via an inverter-controlled variable speed pump that withdraws water from the tail-water tank and pumps it to the upstream end of the flume. Upon re-entering the flume, the flow first passes through a spherical array to dampen water-surface oscillations and reduce turbulence and then passes through a cylindrical array flow straightener to help transition the flow to a more uniform distribution. A McCrometer Ultra Mag® Flow meter (accuracy of ±0.5% of actual flow) located in the center section of the recirculation pipe allows the flow rate to be read off a digital display. A point

gauge, line laser, and video camera were mounted over the experimental section via portable aluminum frame spanning the width of the flume (refer to Figure 6).

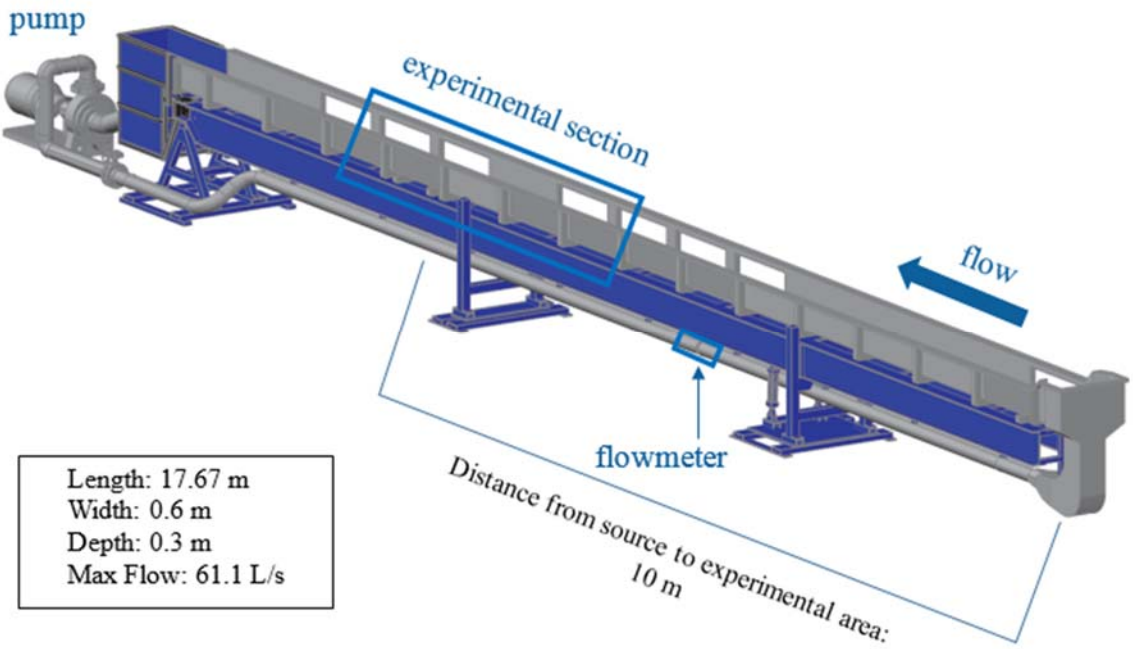

Figure 1: WHOI flume used for unidirectional flow initiation of motion experiments.

Description of the STF:

The STF is an elevated flume that is 19.5 m long, 0.9 m wide, and 0.6 m deep with Plexiglas windows and a painted, rough steel bottom (refer to Figure 2, Figure 3, and Figure 4). Based on flow velocity profiles using a Nortek Vectrino and a log-law fit of the data, the roughness, ks, is roughly 0.047 mm. The flume was temporarily narrowed to 0.55 m wide with cinder blocks and a plastic waterproof covering for these experiments (see Figure 3). A sediment trap at the tail of the flume allows for the collection of any transported material (e.g., munitions) before it gets to the recirculation system. Two screw jacks positioned on either side of a central fulcrum can be used to vary the flume's slope between 0% and 10%. Water is supplied to the flume from the laboratory head tank, and water depth in the flume is controlled by raising or lowering a hydraulic gate at the downstream end of the flume. Flow is controlled by opening and closing the supply valve and is measured with an Ultra Mag ® flowmeter (accuracy of ±0.5% of actual flow). An aluminum frame spanning the width of the flume allowed for a point gauge, line laser, and video camera to be mounted for use in the initiation of motion experiments (refer to Figure 3).

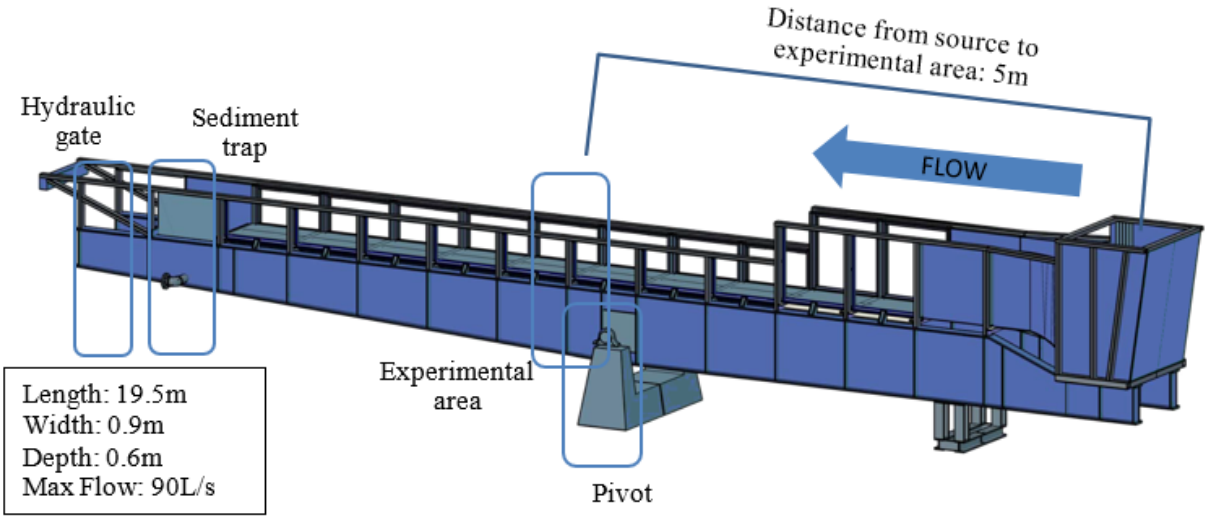

Figure 2: The Small Tilting Flume (STF) was used to continue unidirectional flow initiation of motion experiments from the WHOI.

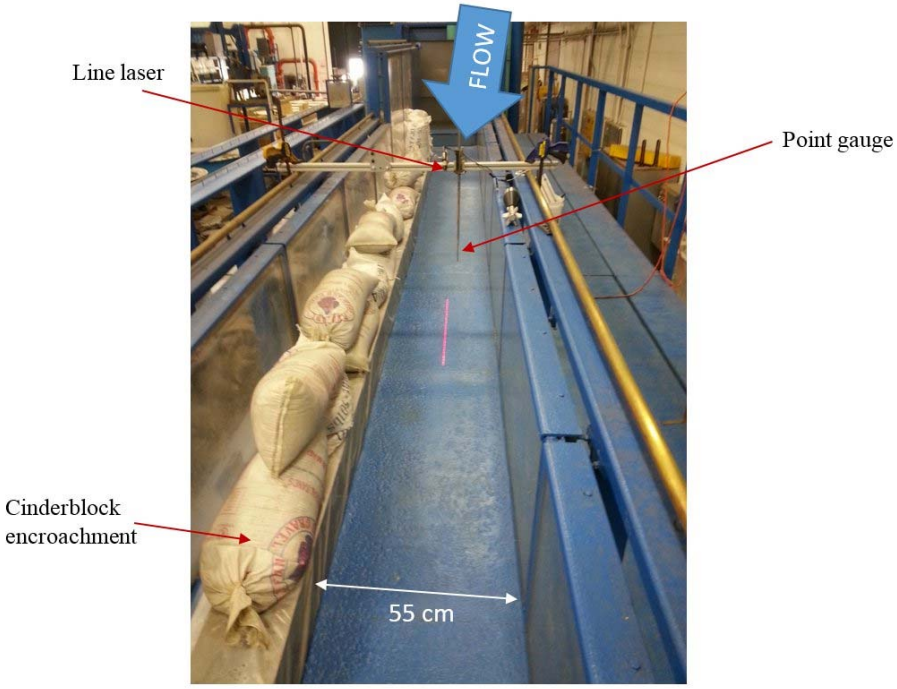

Figure 3: Overview of aluminum frame spanning the width of the Small Tilting Flume (STF) with attached point gauge and line laser. Experiments located 5 m from the upstream of the flume.

Figure 4: The STF bed is made of rough (pitted), painted steel.

Procedure for Initiation of Motion in Unidirectional Flow

Three surrogate munition types (duplicated from surrogates at NRL-Stennis) were used in this study: the 81 mm mortar, 25 mm cartridge, and 20 mm cartridge as depicted in Figure 5. The 25 mm and 20 mm munitions can be separated into two separate pieces, the warhead and the shell casing. "Warhead (or Projectile)" refers to only the stainless steel tip of the munition, detached from the main body. "Casing" refers to the black Delrin plastic body of the munition. "Cartridge (or Round)" refers to the entire munition. The 81 mm mortar can also be separated into two parts, which we can call the "tail" and the "body". "Tail" refers to the aluminum shaft with attached fins. The term "body" refers to the remaining black and metallic projectile (composed of stainless steel and Delrin plastic). The word "finless" is also used to identify the 81 mm mortar body alone (i.e., without the tail). An overview of the six surrogate configurations that were tested can be seen in Figure 5.

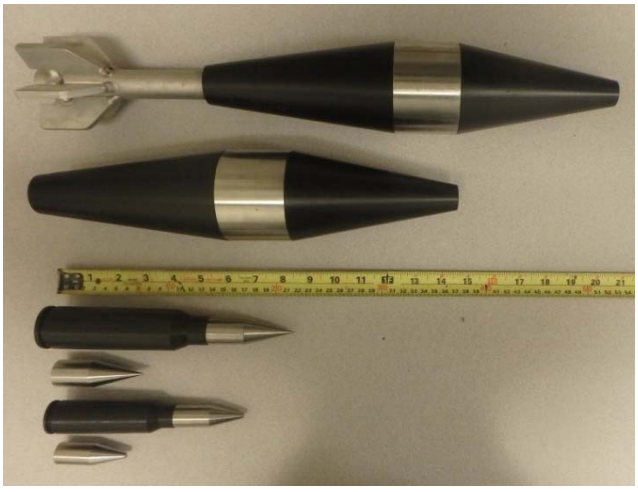

Figure 5: From top to bottom: 81 mm mortar, 81 mm body (finless), 25 mm cartridge, 25 mm warhead, 20 mm cartridge, and 20 mm warhead.

Surrogate Type	diameter [mm]		length [mm]		
	warhead	shell	warhead	shell	total
20 mm cartridge	19.9	29.4	61.1	107.1	168.2
25 mm cartridge	24.8	37.8	78.7	140.1	218.8
	body	fin	body	fin	total
81 mm mortar	367.6	26	357.6	157	514.6

Table 1: Geometry properties of surrogate munitions. Note the fin columns for the 81 mm mortar are grayed out since experiments were not conducted with only the fin section.

Some surrogates manufactured at NRL-Stennis were included in the initiation of motion experiments. Though the NRL and UIUC surrogates are identical in shape and volume, it was found that the smaller NRL-Stennis surrogate munitions had slight higher densities than the surrogate munitions manufactured at UIUC (as seen in Table 2). However, results from initiation of motion testing show the slight difference in density had no significant effect on the motion exhibited in the munitions on smooth PVC substrate. For completeness, any tests conducted with NRL surrogates have been denoted with an asterisk (*) in the graphs included in this report. The NRL munitions were returned to NRL-Stennis before experiments on a horizontal PVC bottom were concluded, and experiments continued using only UIUC surrogates on the rough steel substrate and with a non-zero flume slope.

Source	Surrogate Type	Volume [in^3]	Mass [lb]	Bulk Density [lb/in^3]
NRL	20 mm cartridge	4.7	0.45	0.096
	25 mm cartridge	10.1	0.86	0.085
	81 mm mortar	73.8	8.3	0.112
UIUC	20 mm cartridge	4.7	0.41	0.087
	25 mm cartridge	10.1	0.76	0.075
	81 mm mortar	73.8	8.6	0.117

Table 2: Surrogate properties for the surrogate munitions machined at NRL and UIUC (NRL surrogate properties values from Joe Calantoni).

The examined munition was placed into the flume at a predetermined angle offset from the flow direction as illustrated in Figure 6. Ten angles were tested at 10° increments between 0° (parallel to flow direction) and 90° (perpendicular to flow direction) for each munition. After the munition was set at the proper angle, the flow rate was incremented until either displacement occurred or five minutes transpired without displacement at the maximum flow. When displacement occurred, the bounds of the flow rate interval and their corresponding surface water levels were averaged and recorded. Onset of oscillating motion or rocking with no net displacement was noted, but did not signal the end of a trial. Environmental data such as water temperature, bed substrate, and flume slope were also recorded.

Initiation of motion experiments were initially conducted in the WHOI flume on a leveled bed (0° slope). The maximum average flow velocity produced in the WHOI (0.80 m/s) was not powerful enough to transport any munition during 0° trials. Consequently, experimentation continued in the larger STF, which can produce a slightly higher maximum average flow velocity on a leveled bed (0.90 m/s). To better match the bed roughness conditions in the WHOI, a thin sheet of PVC was installed in the experimental area of the STF for several trials. The sheet was affixed to the dry flume bed using a combination of magnets and plastic tape to smoothly transition flow.

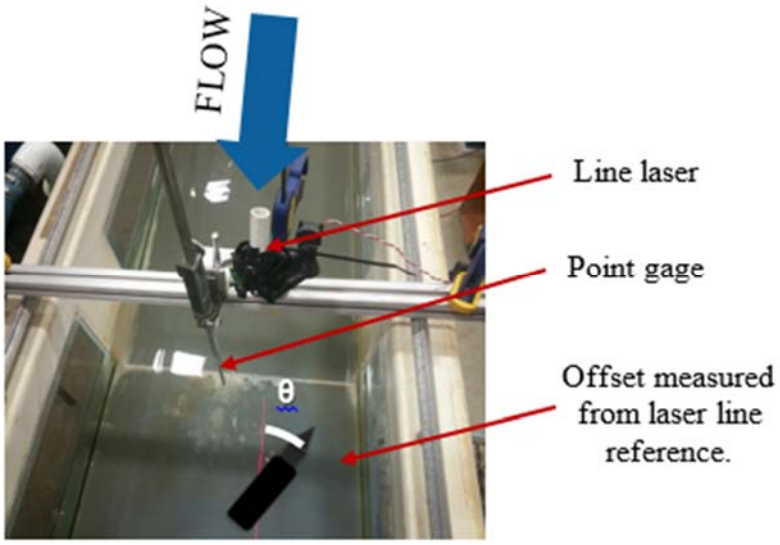

Figure 6: Zoom in on the apparatus in the WHOI flume: an aluminum beam spanning the flume supported a point gauge and line laser. A video camera was mounted above to record trials.

Typical procedural workflow for initiation of motion experiments:

1. Prepare the experimental environment. In the case of the WHOI flume, fill the tank to the predetermined still water height (12.0 cm). In the case of the STF, adjust the gate to the appropriate height. For both flumes, initiate a low flow rate and allow a steady state to establish. Record water temperature. Turn on the line laser and align it parallel to the flow in the middle of the channel. If the trial will be recorded, mount the video camera to the support beam.
2. Check water depth. Submerge the munition in the flume, checking that the water depth is at least twice the height of the munition. If it is not, then adjust the gate height. To avoid surface effects, the water depth was maintained at least twice the height of the munition for all flow rates.
3. Position the munition. Submerge a protractor and measure the appropriate angle from the line laser, using the laser as a baseline. Carefully position the munition along the protractor with the line laser intersecting the munition where the warhead and casing meet. When the munition is set, carefully remove the protractor without disturbing the munition.
4. Perform the trial. After the munition is set, begin video camera recording (if applicable). The frames of the video prove useful in capturing the details of the trial, especially near

the threshold of motion. Slowly increase flow incrementally. Allow time (~20 seconds) between each step for the flow to stabilize in the flume. When munition movement (downstream transport) occurs, record the bounds of the flow intervals and the surface level readings for each. Stop the video camera recording.

5. Repeat steps 2 to 4 at least three times to identify outlier trials. (Sometimes a sudden turbulent burst could disturb the munition before it would move in an ideal current)
6. Repeat steps 2 to 5 for all specified angles for each munition.

Note: It was found that STF could not produce conditions for downstream transport for any of the tested munitions during 0° trials on a leveled bed, so a mild slope (0.4°) was applied to the STF and more trials were conducted. Average flow velocity for all trials was calculated by dividing the flow reading (L/s) by the channel's cross sectional area. This value is also known as superficial velocity. (For reference, a summary table of initiation of motion experiments can be seen in the Appendix, Table 5).

3.1.2 Particle Image Velocimetry (PIV) Measurements

The objectives of our current PIV program can be divided in three parts: I) understanding flow dynamics of fixed munitions; II) performing pivoting analysis for ideal objects, and III) estimating flow around a moving munition. The statuses for the parts I, II and III are work-in-progress, work-in-progress and future-work respectively. For all the PIV measurements, standard 2D PIV will be used.

The PIV procedure described here is applicable to Parts I, II, and III, the only significant difference being the tracer particles used. The tracers used in this experiment are hollow glass spheres with a diameter of 40 microns that can follow the motion of the flow. The tracers are illuminated along the observation plane with a laser sheet that is positioned in the flow. The laser light is scattered by the tracers and captured by a highly sensitive CCD camera. To obtain instantaneous velocity fields, pairs of images of the flow field are taken with a short time separation (order of magnitude 10 milliseconds) by a 4 MP CCD camera. The velocity of the fluid at each grid point in an image is mapped from the average of the velocity of the particles near the grid point. For more information about PIV, please refer to Raffel et al. (1998). The PIV system used in this work contains a New Wave Gemini Nd:YAG laser, Power View 4MP Plus CCD camera, TSI 610035 synchronizer, and optics such as cylindrical lenses, spherical lenses, and mirrors to spread and direct the laser sheet into the flume.

Facilities

Unidirectional flow experiments were performed in the Illinois Hyporheic Flow Facility (IHFF). Oscillatory flow experiments were performed in the Small Oscillatory Tunnel (SOT).

Illinois Hyporheic Flow Facility: The Illinois Hyporheic Flow Facility (IHFF) is a recirculating open-channel water flume that houses a fixed packed bed as shown in Figure 7. The fixed packed bed consists of uniform size plastic spheres that have a diameter of 0.04 m and are arranged in a cubic packing. The test region in the flume is 4.8 m long and has a 0° slope. The rectangular cross section in the test region is 0.35 m wide and 0.3 m high. The munition is fixed on a non-porous sheet that is 0.4 m long and 0.26 m wide and placed above the permeable bed during the

experiments. The munition is aligned with the flow ($\theta = 0$). A transparent visor was placed at the water surface to prevent the surface waves from interfering with the laser sheet.

PIV experiments were conducted in the Illinois Hyporheic Flow Facility (IHFF) to illustrate the flow field around the munition under unidirectional flow when the munition is aligned with the flow on a flat plate. Five tests were conducted in IHFF with different free stream velocities ranging from 0.04 m/s to 0.78 m/s as listed in Table 3 covering the range of flow velocities in which initiation of motion was observed in the WHOI flume or the STF. Results are discussed in the Results section.

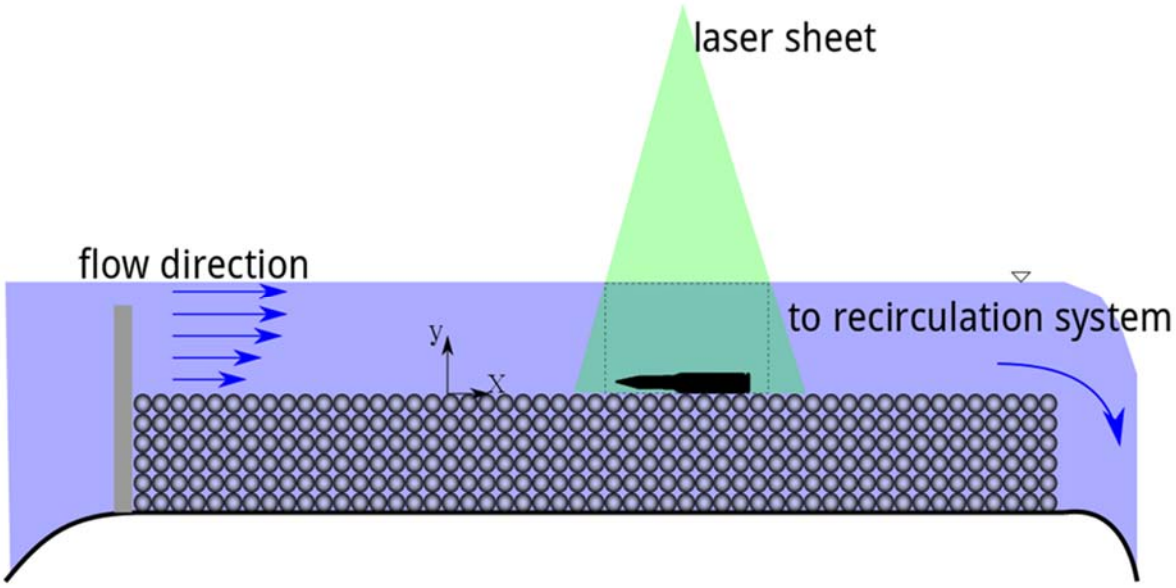

Figure 7: Sketch of the Illinois Hyporheic Flow Facility, side view.

Test no.	Free Stream Velocity (m/s)
1	0.78
2	0.25
3	0.15
4	0.06
5	0.04

Table 3: The conditions of the experiments in IHFF.

Small Oscillatory Tunnel: The Small Oscillatory Tunnel (SOT) is a U-shaped tube that has a length of 3.9 m, a height of 0.25 m, and a width of 0.20 m in the testing section and is shown in Figure 8. A piston located at one end of the U-tube is used to drive the flow toward the opposite end of the tunnel, which is open to the air. Gravity and/or negative pressure at the face of the piston cause the flow to change direction on the reverse stroke, setting up an oscillatory flow condition. Table 4 lists the operating conditions that were run in this set of experiments. The period ranged from 2 to 5 seconds, while the half stroke of the piston is between 0.02 m and 0.1 m.

Experiments were done in the Small Oscillatory Tunnel (SOT) to explore the flow field around the munition under oscillatory flow when the munition is fixed on the bottom. Two cases were examined with munition aligned either perpendicular or parallel to the flow.

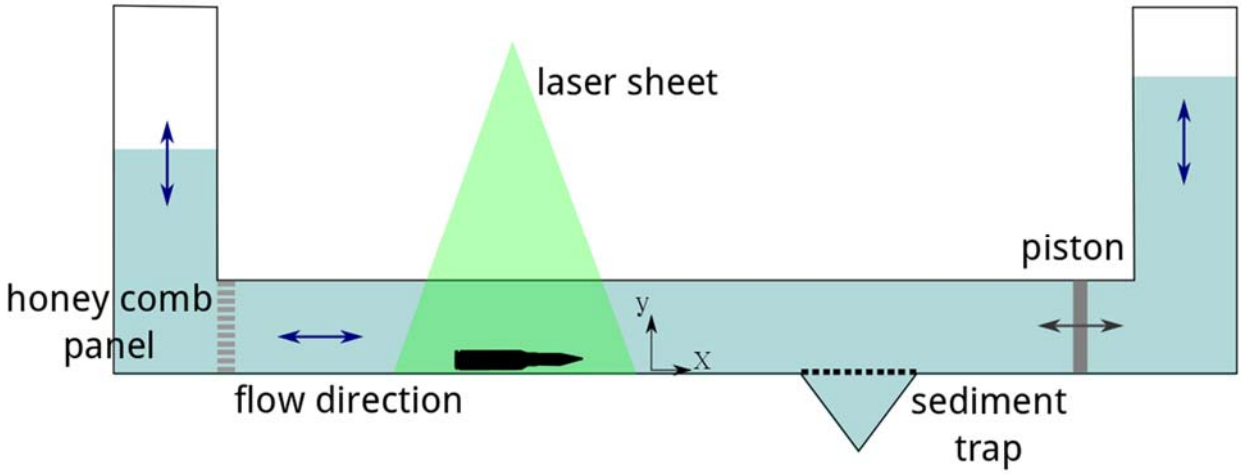

Figure 8: Sketch of the Small Oscillatory Tunnel, side view.

Test no.	Period, T(s)	Amplitude, A(m)
1	5	0.10
2	5	0.06
3	3	0.08
4	3	0.04
5	2	0.04
6	2	0.02

Table 4: The conditions of the experiments in the Small Oscillatory Tunnel.

To construct the mean flow field in three dimensions around the munition under oscillatory flows, PIV measurements were taken at different locations. The measurements were done for six slices when the munition is perpendicular to the flow direction and two slices when the munition is aligned parallel to the flow. The location of the slices on the munition is shown in Figure 9. To date, more than 3 terabytes of PIV slicing image data is being processed to reconstruct the flow field in three dimensions around the munition.

Reflection of the laser light from the munition presented a problem for resolving the velocity field near the munition. To reduce the laser reflection from the munition, the munition is coated with resin that contains Rhodamine WT. The Rhodamine WT paint absorbs the green laser light (wavelength of 532 nm) and emits a light with a different wavelength (545 nm). Applying a band pass filter on the camera lens allows the green light scattered by the PIV seeding particles to be seen by the camera but filters out the 545 nm reflection from the Rhodamine WT coating applied on the munition.

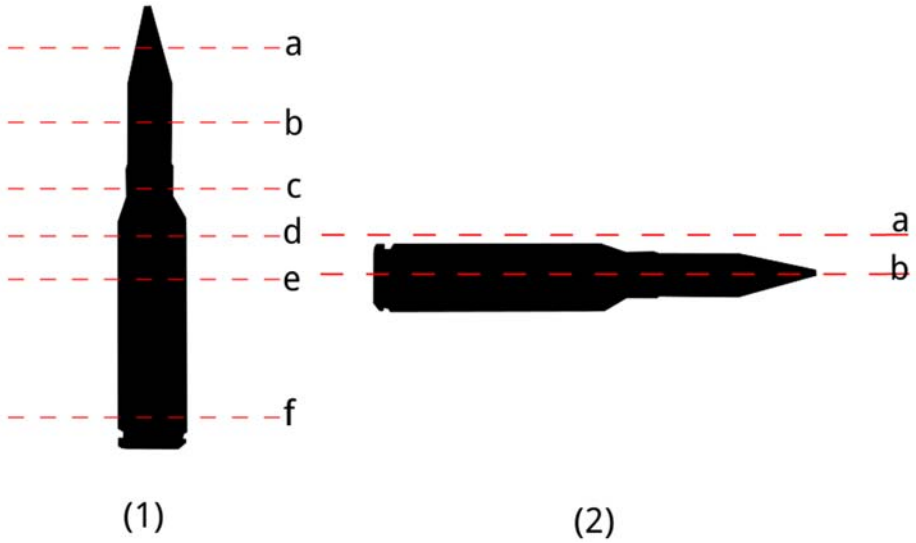

Figure 9: The top view of the locations on the munition where the slices of PIV measurements were taken. “Slice a” is the closest to the camera.

Part I: Understanding flow dynamics of fixed munitions

Part I is conducted to obtain the flow field measurements of munitions fixed to the bottom of a channel to gain insight on the flow dynamics around the munition. For this portion, we perform PIV measurements of the fixed munition in a unidirectional channel and in a small oscillatory tunnel. From the PIV measurements, we have the instantaneous flow velocity fields. With these velocity fields, we can calculate the mean flow velocity fields and the vorticity that can indicate the flow separation zones, relevant in erosion effects. The PIV data shall also aid in the estimation of the forces on the munition and calculation of drag coefficients which can be used to better understand and predict munition migration.

Part II: Pivoting analysis for ideal objects

The second objective is to perform pivoting analysis for ideal objects (spheres and cylinders) over idealized rough beds. The analysis of these experiments on ideal objects is performed following the work of Komar and Li 1986, where the scaling to which they arrived is illustrated by Figure 10. In that figure, a moment balance is performed taking in consideration just two forces: shear driven drag and immersed weight. The Shields-like object mobility parameter that is obtained following this approach is inversely proportional to the size ratio of the pivoting particle and the rough bed. The PIV experiments are needed here to estimate wall shear velocities in imminent motion of spheres and cylinders. The way we estimate the shear velocity is by approximating it to the maximum value of Reynolds stress. These tests for idealized geometries will allow us to ascertain that our approximation of shear velocities for highly rough walls is appropriate.

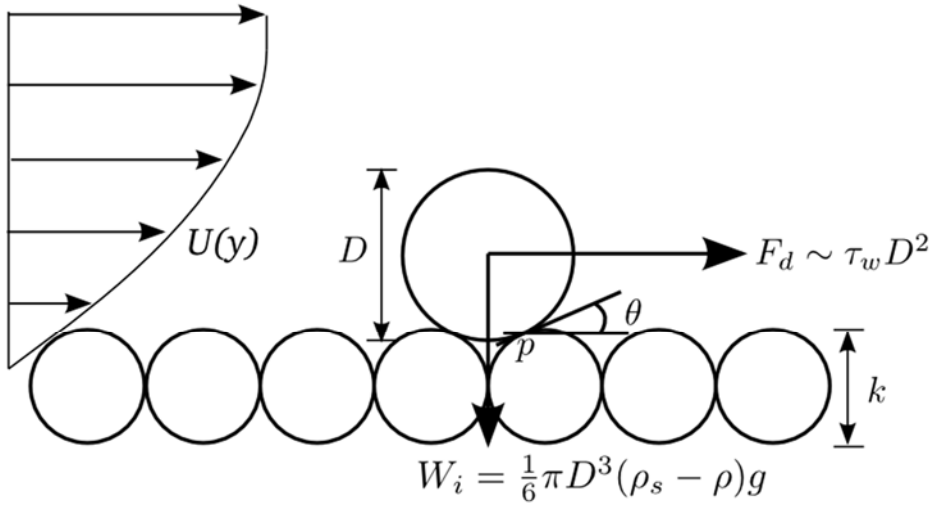

$$\text{for large } (D/k),\ \frac{\tau_w}{(\rho_s-\rho)gD} \sim (D/k)^{-1}$$

Figure 10: (Adapted from Komar and Li 1986) Schematic of a pivoting particle of size D lying on a rough bed with roughness elements of size “k”. Two forces are present at the instant of imminent motion, shear driven drag (Fd) and immerse weight (Wi). A moment balance around the contact point “p” is done which includes the two forces arriving to the relationship that the object mobility parameter is inversely proportional to the ratio D/k.

Part III: Flow estimation of moving munition.

The last objective of our flow measurements is to get PIV results for a munition at the instant of imminent motion. The reason is to observe the flow dynamics around the munition at the instant of imminent motion and when the munition is moving while tracking the motion of the munition itself with other techniques (e.g., electronically with the IMU). These measurements will be performed in oscillatory flow conditions. Our intent is also to use the data generated in this portion and to compare it to the plots generated by Friederichs (2013). Note that Komar and Li (1988) have a model that is very similar to the one by Kirchner et al. (1990), used by Friederichs. The models indeed arrive to an almost identical balance equation. The main difference between the Komar and Li and the Kirchner et al. model is that Komar and Li includes a turbulent fluctuation factor that accounts for the direct effects on velocity fluctuations in the imminent motion of solids.

3.2 Development of Motion Capture Techniques

The movement of a rigid body in space can be decomposed into six unique motions (x-, y-, and z-translation, pitch, roll, and yaw). In the case of the submerged munitions, motion is usually a composition of many of these six movements. As such, determining and recording even a small amount of movement by hand can become prohibitively time-consuming. In addition, while the movement of the cartridge between two locations and orientations is unique, it cannot be uniquely decomposed from discrete data. To ensure a faithful account of munition movement, it is necessary to sample and record the state of the munition at a high rate, something that yet increases the time cost and complexity of recording manually. Automated tracking represents a solution to these problems in that it can rapidly record small changes in position with a high temporal resolution.

3.2.1 Motion reconstruction from Feature Tracking

Reconstructing the full Lagrangian description (translational and rotational motion) of a rigid body can be achieved by performing stereoscopic tracking of visual features present on the surface of the object of interest (Zuniga Zamalloa, 2014). The crux of the method lies on adding color texture (henceforth referred as texture) to the object to be tracked, which in the present experiments is a munition. Here, a process similar to the preparation of specimens in Digital Image Correlation is used to create a speckle pattern on the surface of the munition (see left panel of Figure 21). First, a thin coating of paint (e.g. white) is applied to the munition. Then, a random monochromatic pattern is added in a contrasting color (e.g. black). The added texture on the munition generates several distinct features across the surface of the object. These distinct features are used as non-repeatable markers whose displacement is tracked, thereby allowing the reconstruction of the motion of the particle.

The steps of feature detection and tracking in the images is done following the work of Lowe (2004). The latter allows us to work with features that are scale- and rotation-invariant, therefore reducing errors due to high speed rotation and out of plane motion. The three-dimensional reconstruction is obtained by using a stereoscopic system of two identical high-speed cameras with a 4 MP resolution, conditioned with 28 mm lenses. Four 500 W halogen lights are used to reduce the shutter time in the cameras and in doing so, improve the quality of the images. The munition

used for the present experiments was a 20 mm munition. A schematic of the setup is shown in Figure 11.

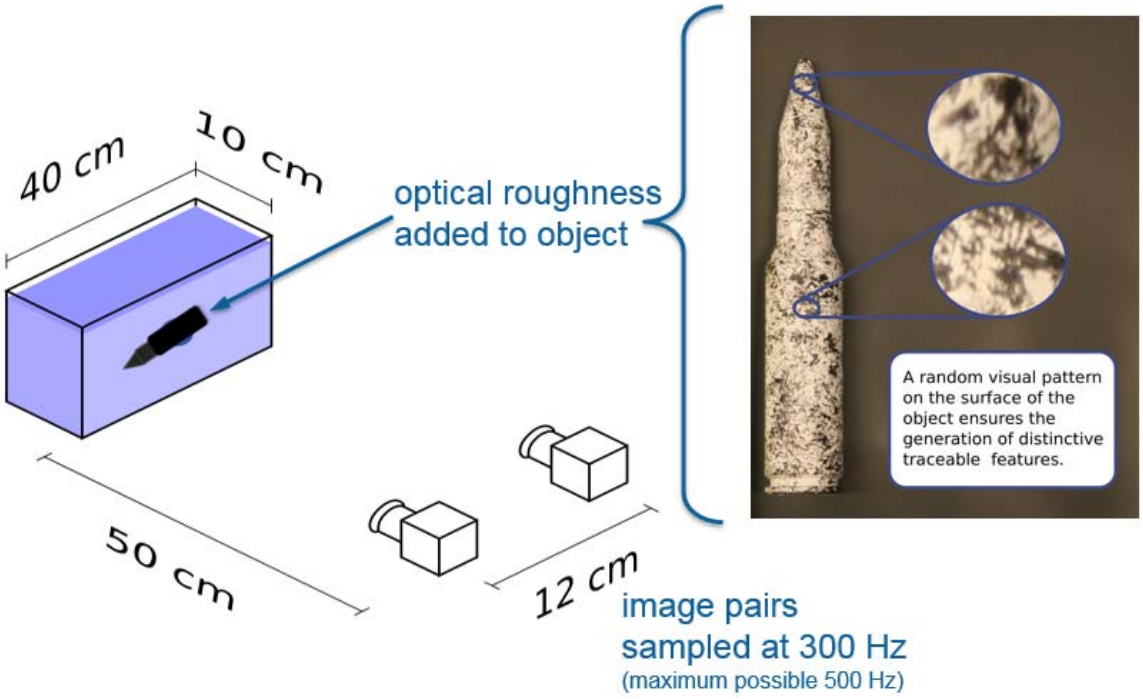

Figure 11: A schematic of the experimental setup used to perform feature tracking on a 20 mm munition with added color texture to retrieving six degrees freedom.

Once the set of features and their three-dimensional positions at different instants of time are available, the displacement of the points in the point cloud is used to obtain translation and rotation. Using principles of rigid body mechanics (the munitions can be considered rigid in the present experiments) the motion of an object can be decomposed into pure translation and rotation. The rotational motion is obtained by fitting a rotation matrix to map the position of the features at one point with the position of those same features at a consecutive instant of time. By performing a least squares fit to the prescribed rotation matrix given the displacement of the features, one can obtain the unit-vector with the direction of rotation and the angular displacement itself.

3.2.2 Structure from Motion (SfM)

Structure from Motion (SfM) is a technique used to generate three-dimensional structures from a set of two dimensional images. In brief, SfM entails searching images for distinguishing features, pairing images who share a common feature, and then creating a point cloud. It is similar in principle to techniques used by the human brain to reconstruct 3D images when viewing an object in motion with one eye closed. This method not only can reconstruct the munition in 3D but can reconstruct the surrounding bathymetry as well. Provided that image sets are acquired at time intervals throughout an experiment, a time resolved 3D reconstruction can be created.

Two programs were used in testing the feasibility of SfM as a method of object tracking: VisualSfM and Agisoft PhotoScan.

Visual SfM

Visual SfM is a professional level 3D reconstruction Graphical User Interface (GUI) created by Changchang Wu in 2013. Agisoft PhotoScan is a self-contained, proprietary photogrammetric program. Both Agisoft Photoscan and Visual SfM require the user to input a series of photographs (or frames from a video) of an object or environment. Visual SfM allows the user to find paired images, and reconstructs a sparse point cloud and dense point cloud. To create a mesh, the cloud must be saved and transferred to MeshLab, a free program for processing 3D meshes. To apply texture, the mesh can be saved and imported to Blender, a free, open-source computer graphics software. The process of cleaning meshes imported from Visual SfM to Meshlab can be time intensive for the user. Finally, the resulting point cloud can be scaled in Visual SfM to convert the points to real world coordinates.

Agisoft

Agisoft Photoscan, which is completely self-contained, eliminates the need to import to multiple programs. Agisoft Photoscan Professional allows construction of grounded models. Agisoft is a commercial software package where as VisualSfM is currently freely available.

4. Results and Discussion

4.1 Laboratory Experimental Results

4.1.1 Initiation of Motion Results in Unidirectional Flow

Several different types of motion were observed in the initiation of motion experiments depending on the type of munition tested and its orientation to the flow, as depicted in Figure 12 and Figure 14. For cartridges at nonzero angle offsets, motion followed the path of a rolling cone. This is because the cartridge weight is distributed over two edges with different diameters: one edge on the munition head, and another on the casing (these contact points are denoted as orange points on the top image of Figure 12). Warheads roll in a linear motion because their weight bearing surface has a uniform diameter (contact points are denoted with orange lines in the bottom image of Figure 12).

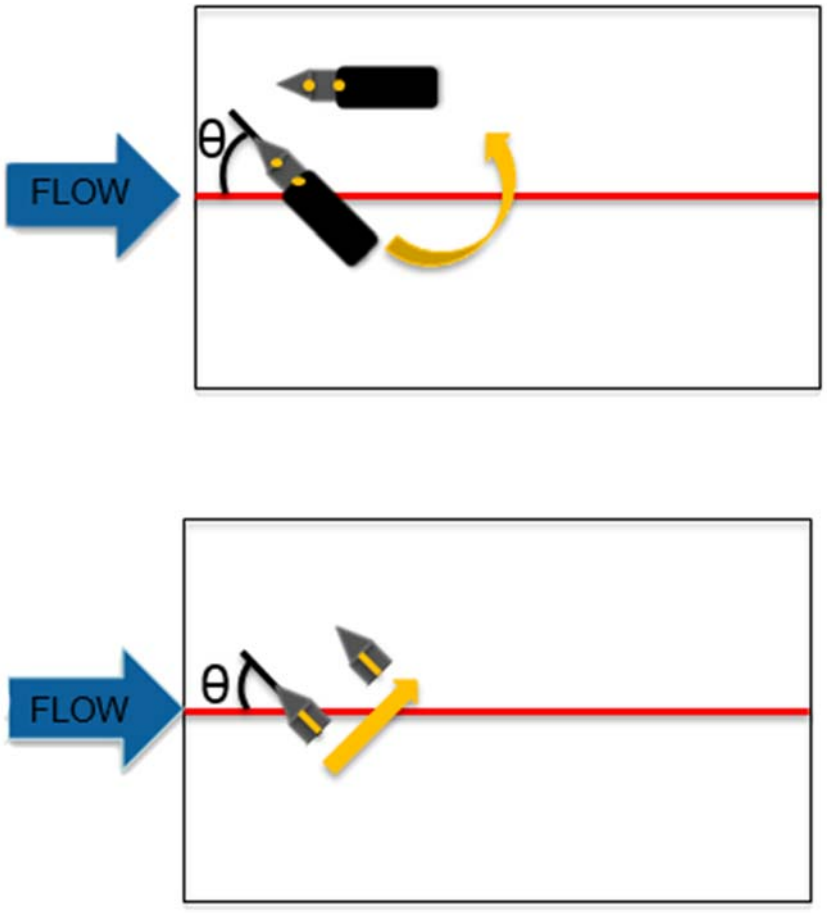

Figure 12: Schematic of initial motion behavior for cartridges (top image) and warheads (bottom image). Cartridges rolled on two weight-bearing points in a conical motion. Warheads rolled linearly on a cylindrical weight bearing surface (weight-bearing contacts indicated by orange points or lines).

The results of initiation of motion experiments performed in the WHOI show a clear relationship between the angle to flow, and the amount of force required to move the munition (see Figure 13). As the cartridge and warheads approach an angle of 0°, less of the munition's surface is exposed to the flow. Thus, as this projected area of the munition decreases, the velocity necessary to initiate transport increases. Motion could not be achieved for any munition or warhead in the WHOI flume when placed parallel to the streamwise direction ($\theta = 0°$), prompting experiments to be moved into the STF.

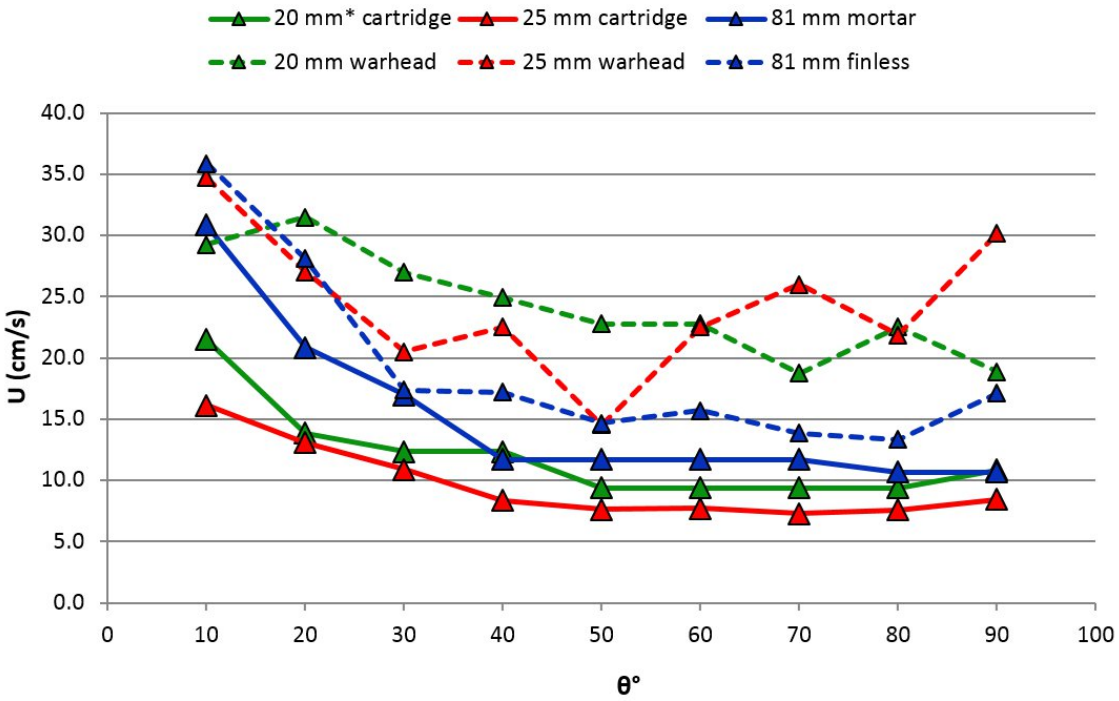

Figure 13: Initiation of motion for munitions and warheads on a horizontal PVC bottom. Note the * denotes that the NRL surrogate used.

Initiation of motion of the munition when placed in line with the streamwise direction ($\theta = 0°$) could not be achieved in the WHOI flume. The width of the flume was not reduced by encroachment in the WHOI flume because the flume walls were not deep enough to accept the resulting increased water depth. Therefore, experiments were continued in the STF, which is both deeper than the WHOI and can produce a slightly more powerful flow.

During $\theta = 0°$ trials in the STF, it was found that none of the munitions could be moved on a horizontal bed (slope=0.04°, taken as a horizontal bed) on the flume's original rough steel. A smooth PVC patch (material similar to the WHOI bottom) was installed. This also failed to yield transport when placed at $\theta = 0°$, even at the highest flow velocity available to the STF (maximum flow velocity of 0.91 m/s). However, rocking movements were observed when high flow rates were applied to munitions placed at $\theta = 0°$ on both the steel bottom and PVC patch.

At this point, a mild slope was applied to the STF (slope of 0.4°). With this slope, the 20 mm and 25 mm cartridges in $\theta = 0°$ trials achieved stochastic downstream transport on the PVC patch

during high flow rates, with initiation of motion becoming more likely as flow was increased. The observed stochastic transport of the 20 mm and 25 mm munitions occurred in three ways:

1) The munition rocks in the violent flow, moving a small distance downstream with each rock (< 1 mm), see top image in Figure 14.
2) The munition suddenly slips downstream a short distance before coming to an abrupt stop (see middle graphic in Figure 14).
3) The munition slips downstream a short distance, but becomes slightly misaligned with the flow and rolls violently downstream on an angle (refer to bottom image in Figure 14). As flow rate increased, motions described in observations 2) and 3) became significantly more likely to occur.

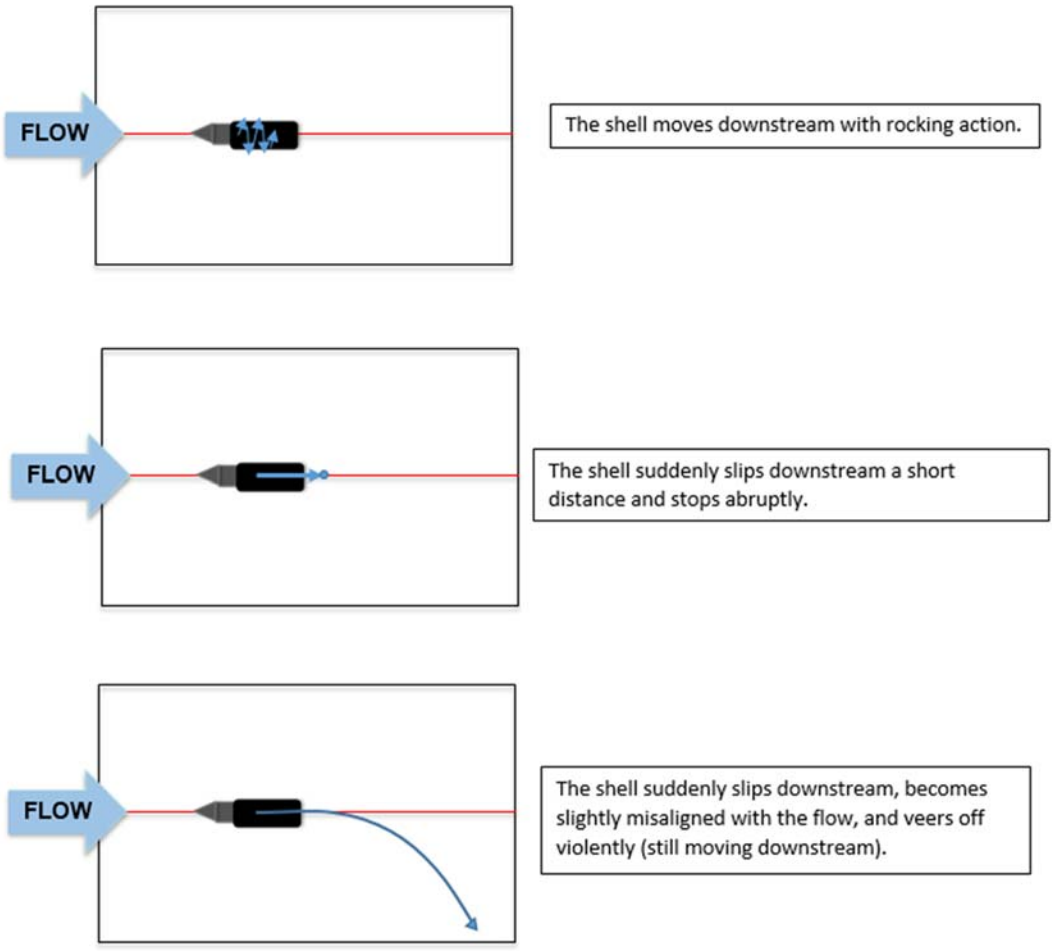

Figure 14: Overview of observed transport behaviors over PVC patch in STF (observations 1, 2, and 3 are listed from top to bottom).

Offset cartridge trials were conducted in the STF on both the horizontal and mildly sloped beds with rough steel bottoms (see Figure 15). The results of shell offset trials on steel bottom in the STF with and without slopes are very similar to each other. We expect that the local roughness of

the steel bed around the munition is enough that the munitions are held in place by individual bumps and divots in the steel. The steel provided enough traction for the cartridges to be set reliably, and yielded a similar relationship between angle and motion-inducing flow velocity to the results found in the WHOI on smoother PVC bottom. Due to the increased roughness between steel and PVC, trials on steel required greater flows as can be seen in Figure 16.

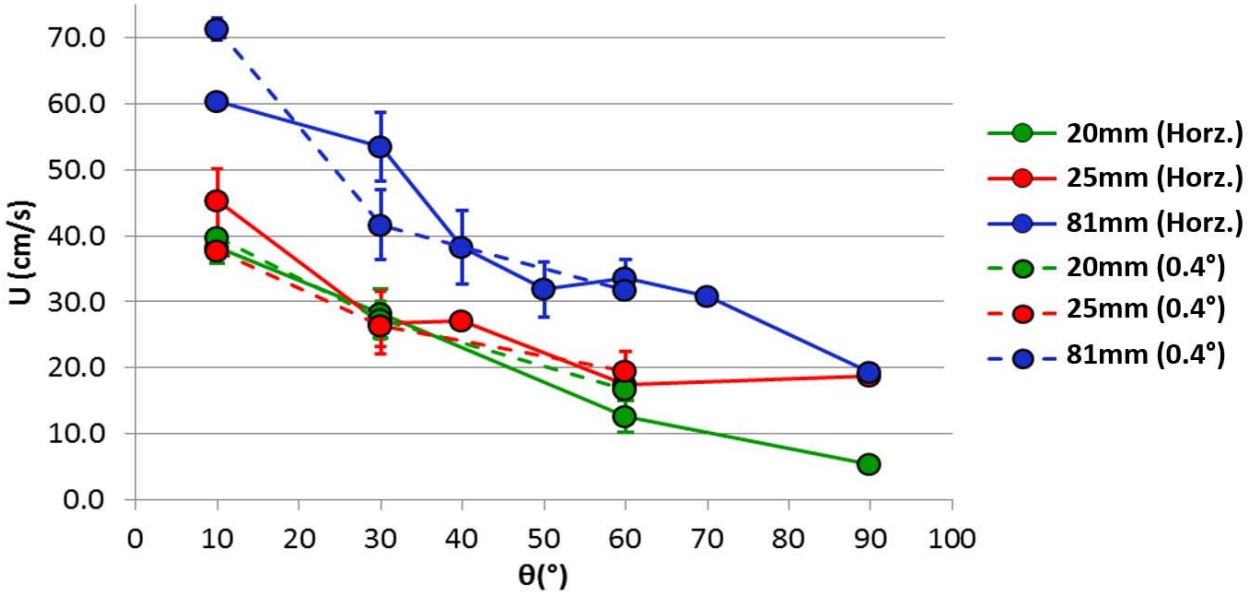

Figure 15: Effect of steel bed slope on cartridge offset trials. Two flume slopes are a mild slope of 0.4° and horizontal slope (Horz.) (slope of 0.04°, taken as horizontal).

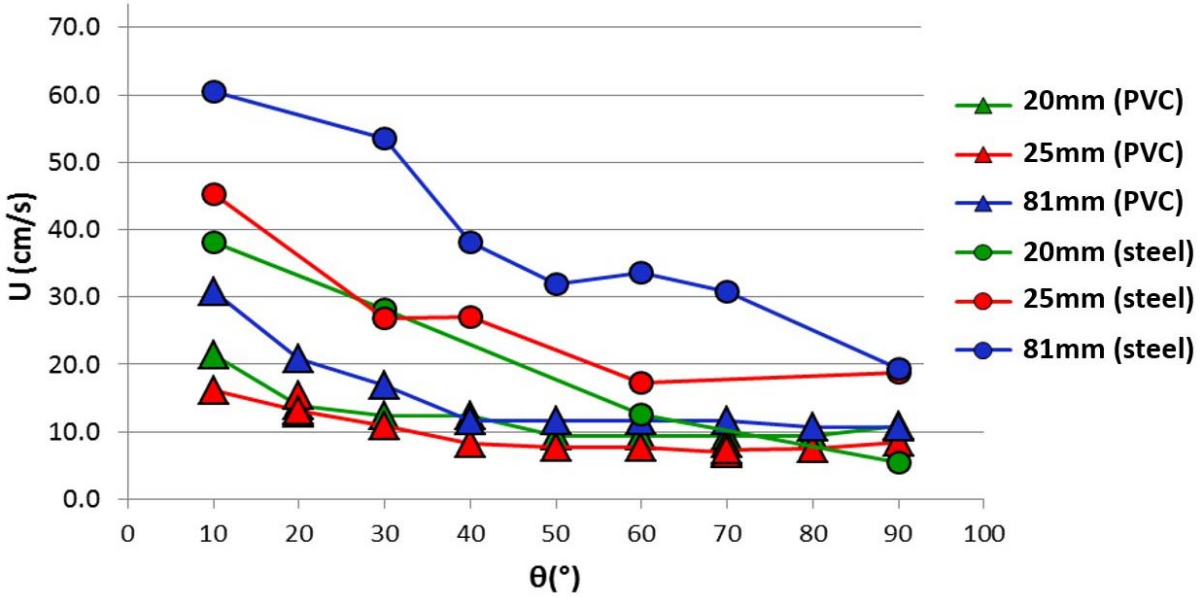

Figure 16: Effect of horizontal bottom rough on cartridge initiation of motion. WHOI flume was used for PVC bottom and STF was used for the steel bed.

Figure 17 depicts current experimental data (previously plotted in Figure 13, Figure 15, and Figure 16) to prior data compiled by Friedrichs (2013). It can be seen that current data regarding surrogate munitions is within the range of scatter of the prior data for spheres, cylinders, and natural sediment. Also, the current data provides a plausible reason for the spread in the data for each diameter; the initiation of motion velocity threshold is highly dependent on the angle of attack of the munition.

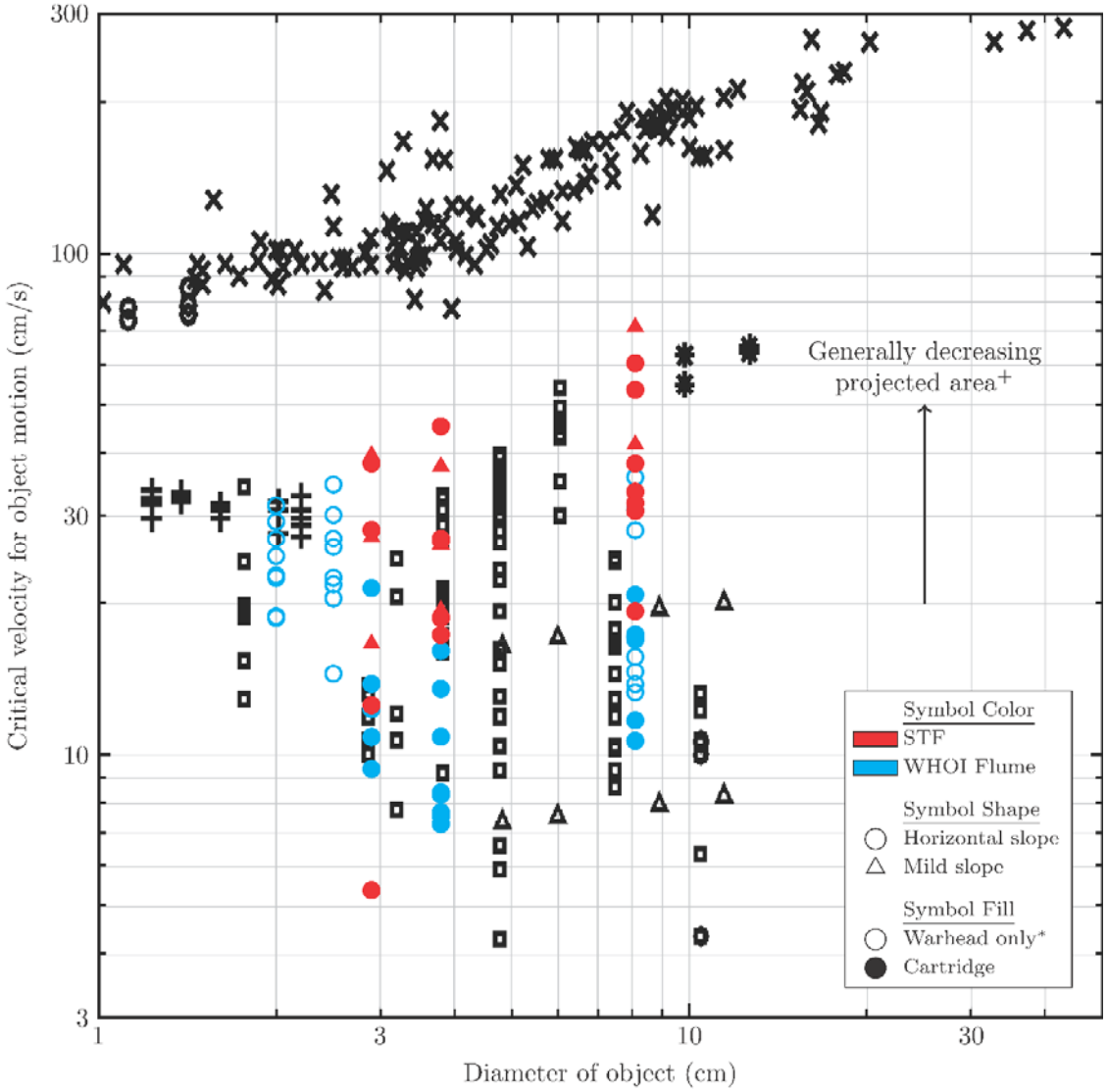

Figure 17: Comparison of the current IOM experiments (from Figure 13, Figure 15, and Figure 16) to data compiled by Friedrichs (2013). Black symbols are prior data from Friedrichs (2013), and red and blue symbols are from current experiments. Symbology can be interpreted as follows: a light blue open circle is a data point collected in the WHOI Flume with a horizontal slope and the warhead only. A filled red triangle is a data point collected in the STF with a mild slope using the whole UXO cartridge. (+ Generally decreasing projected area only applies to data collected by UIUC for the current effort. * The warhead only for the 81 mm UXO is with the fins removed).

4.1.2 PIV Measurement Results

Results for Part I: Understanding flow dynamics of fixed munitions

PIV results for mean streamwise velocity and vorticity are plotted in Figure 18 and Figure 19, respectively, for the unidirectional flow experiments performed in the IHFF. Five different flow velocities are shown in each figure. The munition is aligned parallel to the flow for all five cases and the laser sheet is aligned with the centerline of the munition. In these figures, the free stream is flowing from the left to the right. Figure 18 shows the contours of the mean streamwise velocity fields. The flow is faster in the upper region away from the munition. In the wake region downstream of the munition, the flow is in the reverse direction. To better illustrate the shear between the wake region and the flow above the munition, the vorticity was calculated as shown in Figure 19. The vorticity is close to zero in the free stream. There is a tail of strong vortices immediately behind the munition. The strength of the vortices decreases as the free stream flow velocity decreases.

In addition to the unidirectional flows examined in the IHFF, PIV experiments were also carried out in the SOT for oscillatory flows. The experiments in the SOT are complete and data processing is still in progress. Figure 20 shows a sample of the phase-averaged streamwise velocity field. Phase-averaged streamwise velocity is calculated by averaging the streamwise velocity fields at each specific phase in the piston cycle. The test shown here is “slice d” (refer to Figure 9) of the munition aligned perpendicular to the flow direction. The oscillatory flow period is 3 seconds and a half stroke is 0.04 m. Twenty image pairs were acquired per piston cycle. In Figure 20, it can be observed that the free stream flow is a sine wave. The flow velocity field near the munition is well resolved. The region just above the munition has the fastest streamwise velocity that increases and decreases with the speed of the free stream flow. On the downstream side of the munition, the flow is reversed. The region with a reversed velocity grows as the free stream velocity decreases. In the future, we plan to better identify the regions by calculating the vorticities at the various phases in the oscillations.

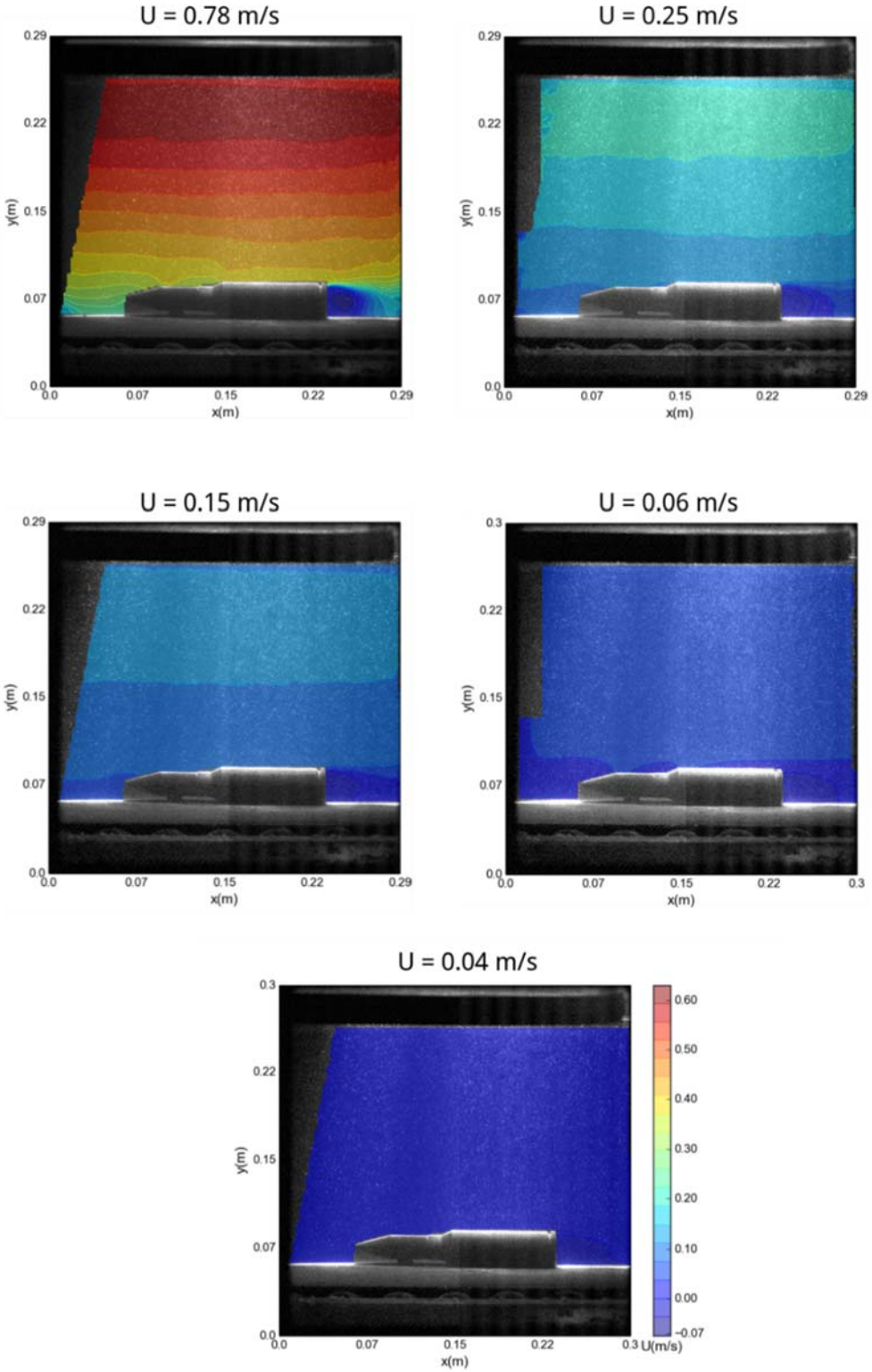

Figure 18: The contours of the mean streamwise velocity field around the munition across the centerline under five different free stream flow velocities (shown in Table 3). The velocity is defined to be positive to the right.

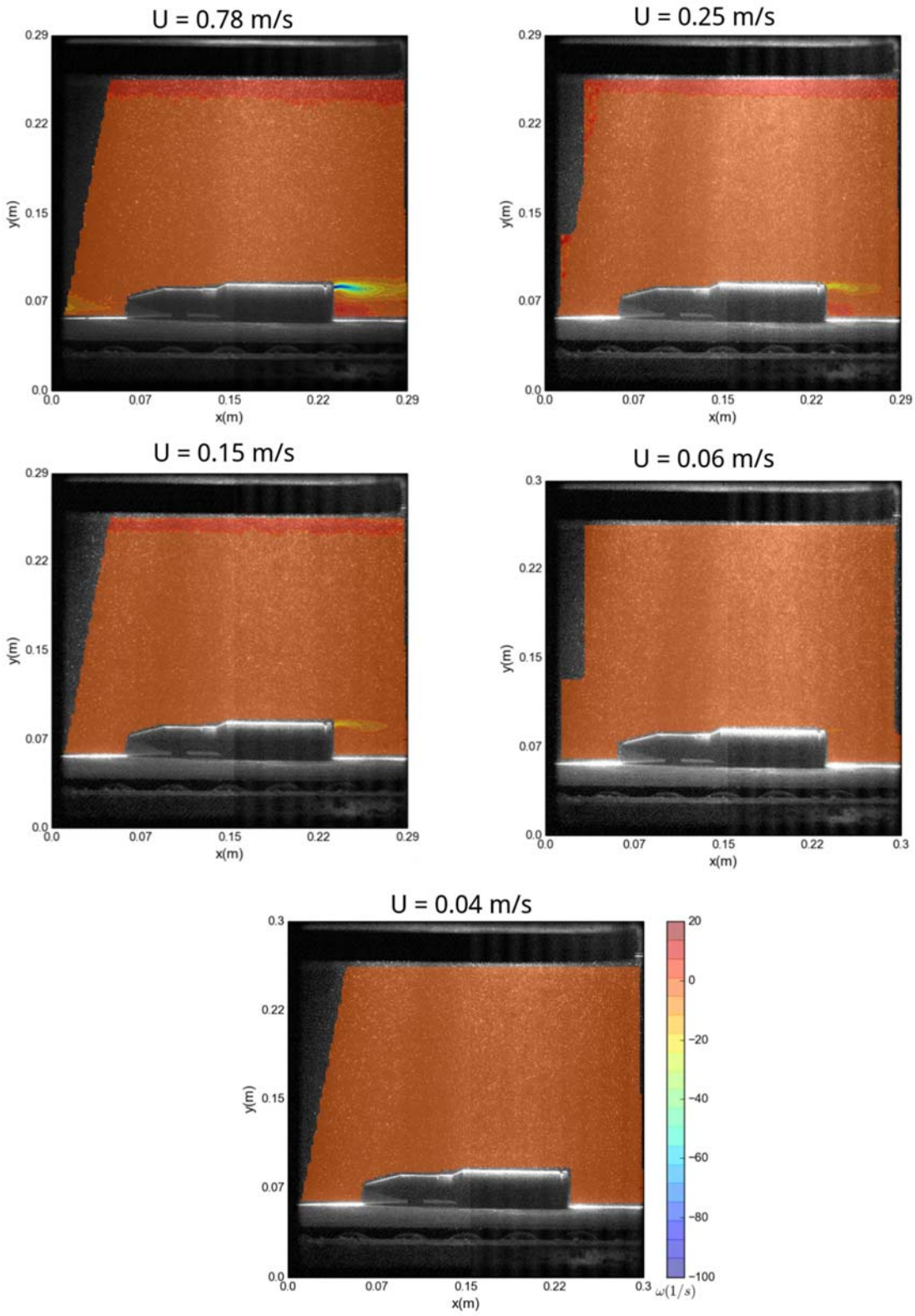

Figure 19: The vorticity around the munition across the centerline under different free stream velocities (shown in Table 3). The positive vortex is counterclockwise.

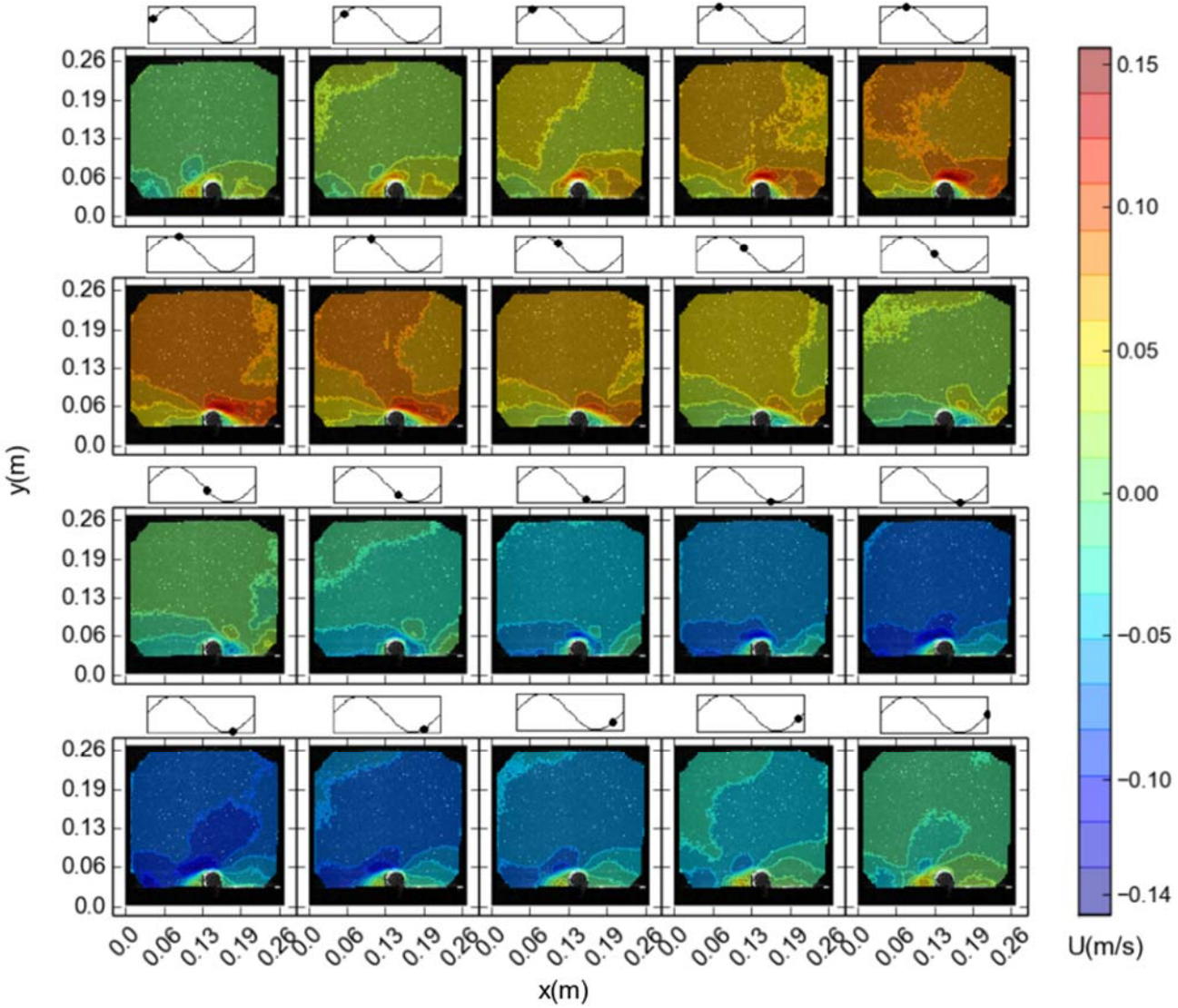

Figure 20: The contour of the streamwise mean velocity at each phase in a cycle. In this test, the period of the piston is 3 sec and the half stroke is 0.04 m

4.2 Motion Capture Techniques: Preliminary Results and Discussion

4.2.1 Motion Reconstruction from Feature Tracking

Following the method outlined on page 13 for retrieval of translational and rotational motion via feature tracking, we are able to obtain the rotation and translation of the munitions for the SERDP project as long as we have optical access.

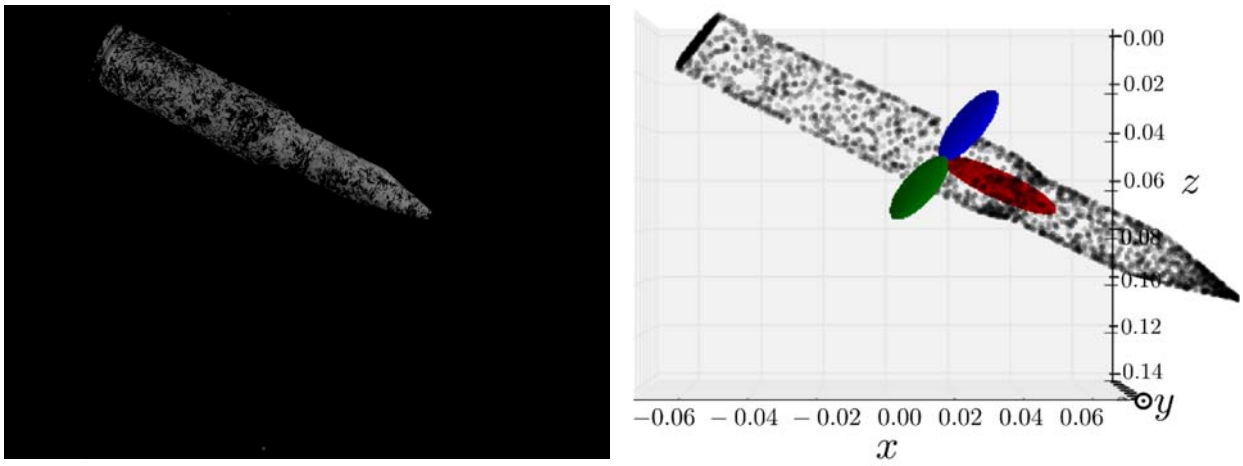

Figure 21: Left panel: A monochromatic speckle pattern is added as color texture on the surface of the munition generating unrepeatable features. Right panel: The unrepeatable features are tracked in space and time using a feature tracking algorithm on the image pairs obtained with a stereoscopic setup consisting of two high speed cameras.

The six degrees of freedom that correspond to translation and rotation can be determined. Three of the six degrees of freedom, the ones that correspond to translation, are presented in Figure 22 as an example of the results. The algorithm allows even the detection of impacting motion (identifiable by the discontinuities around 0.17 seconds in Figure 22). A major benefit of this tracking technique is that it can retrieve the motion for either small or larger specimens. Both large in-plane and out-of-plane components of the translation and rotation can be reconstructed with a good level of accuracy. The technique has the processing time as the only clear limitation if a real time application is sought. Currently, in order to process 800 images (4 MP each) we need around 12 hours.

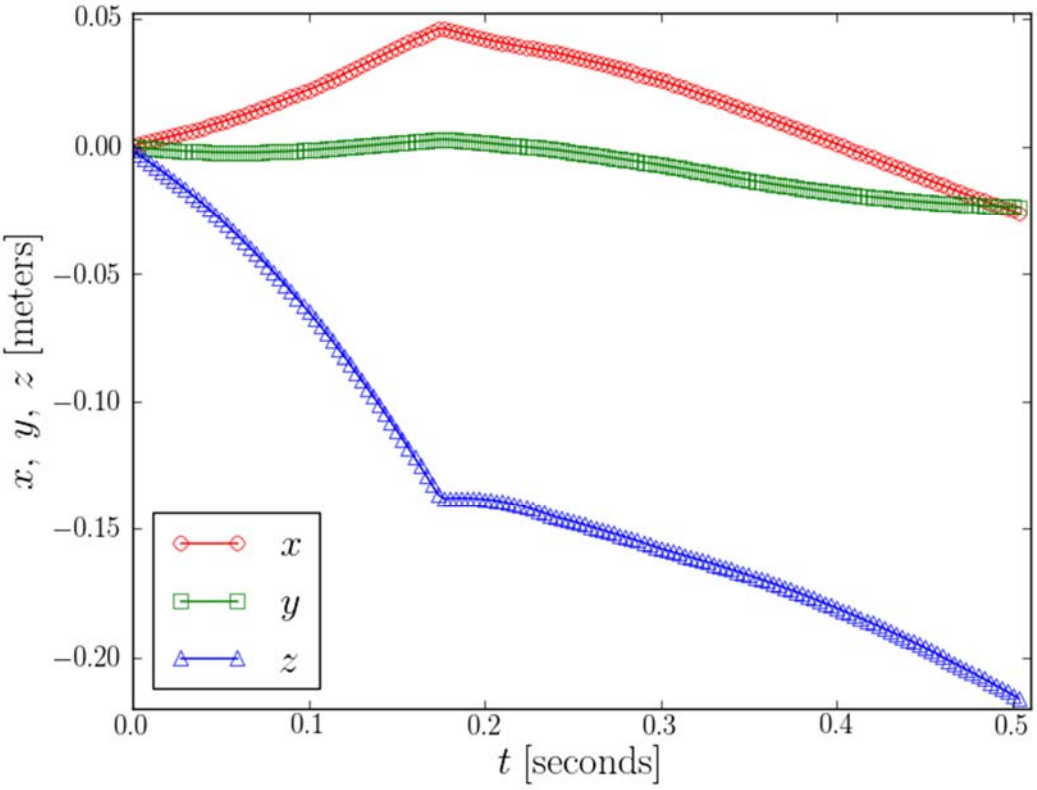

Figure 22: The three components of the translational motion of a 20 mm cartridge falling in a water tank are shown. Note that the impact of the munition hitting the bottom of the tank is accurately detected by the algorithm and is shown in the present plot as discontinuities in the slopes of the three components of the translational trajectories.

4.2.2 Structure from Motion Results

Extensive trials were conducted to determine the suitability of VisualSfM for reconstructing the munition within LOWST. The results of these trials have shown that the freely available VisualSfM software package does not appear capable of reliably reconstructing the experimental area with the geometric constraints imposed by LOWST with respect to viewing window size and location. The commercial AgiSoft software does appear capable of reconstructing the munition within LOWST (Figure 23).

Preliminary results suggest the process is optimized with ten cameras placed in a specific configuration. Eight Network IP (Internet Protocol) cameras were mounted along the two side windows of LOWST (four cameras per window) and two additional web cameras encased in a small watertight enclosure and mounted inside the tunnel directly above the experimental area.

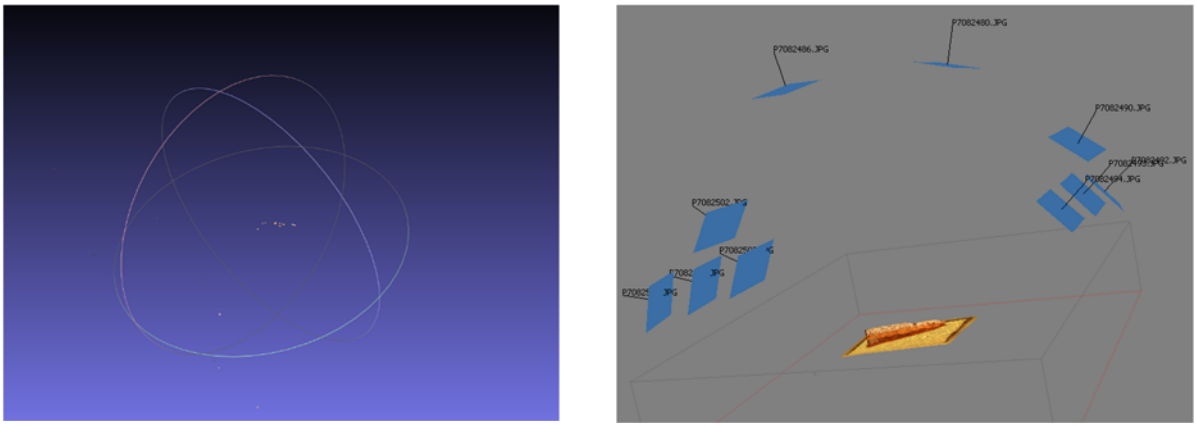

Figure 23: Results from Structure from Motion software packages using the same 10 images for reconstruction of the 20 mm munition: VisualSfM results (left image); AgiSoft results (right image). Blue planes in right image denote relative camera positions for each of the ten images used in the reconstructions.

5. Conclusions to Date and Future Directions

Initiation of Motion Findings on Hard Substrates

Under unidirectional flows over a hard substrate, all experiments show a strong dependence on attack angle (θ) on the mean flow velocity required to initiate motion. For most munitions tested at a non-zero attack angle, this relationship is most pronounced between 10° and 40°, as seen in Figure 13. The type of motion exhibited by cartridges and warheads was distinct. Warheads rolled in a linear path on their long side with constant radius. Cartridges rolled at two points of contact as seen in Figure 11. The radius of the cartridge at the point of contact nearest the munition tip was smaller than the point of contact toward the middle of the cartridge. This caused the munition to rotate its orientation as it rolled. That is, the munition would roll and rotate, eventually coming to a stop at an orientation that was different than its original angle with respect to flow direction. The warhead munitions retained the same, or almost the same orientation with respect to flow direction. Although addition of a mild slope was sufficient to allow for initiation of motion when munitions were placed at $\theta = 0°$on smooth PVC, the mild slope had no noticeable effect on munitions when compared the other tested scenarios: munitions on a rough steel bed and on a horizontal PVC bed. Munitions tested with attack angle of 0° exhibited types of motion and transport (Figure 14) which were not observed in any offset trial (i.e., 10° to 90°). Because of these motion differences, the term "initiation of motion" had to be redefined for 0° trials. In offset trials, the onset of motion was clear – although rocking may have been present, it did not appear to contribute greatly to munition translation. Trials with a 0° angle of attack frequently vibrated or rocked, inching back slowly with each tiny oscillation. All these motion differences made direct comparison of 0° trials and offset trials difficult. The greater the projected area of the munition exposed to the oncoming flow, the lower the flow velocity required to initiate motion. The results are amplified for rougher substrates (e.g., steel versus PVC bottom) as can be seen in Figure 16. Furthermore, the results of these initiation of motion experiments begin to characterize the Lagrangian transport and fate model for munition movement as well as help define experimental parameters for future use in

hard substrate oscillatory flow experiments which will occur in the Large Oscillatory Water-Sediment Tunnel (LOWST). In addition, these experiments have provided valuable insight into the nature of submerged munition movement and how best to implement algorithms to track, classify, and model munition motion.

PIV measurements

For the present PIV experiments with the munition, the velocity scales in the free stream and the wake of the munition are one order of magnitude apart. To resolve the turbulent dynamics in the wake and the rest of the flow, a large effort was put to find the optimum PIV straddling time. Regarding observed flow dynamics in the SOT during PIV experiments, flow separation (vorticity generation) always originated at the base of the munition (i.e. the plane where the primer is located). This separation was irrespective of the direction flow with respect to the munition orientation. This information of vorticity from the SOT experiments will be studied aiming at relating the flow dynamics to the motion of the sediment around the munition.

In the future, in addition to the PIV measurements with the munitions, we will also conduct experiments to further examine the pivoting model in sediment transport. PIV measurement will be done in the IHFF to measure the flow field around cylinders and spheres at incipient motion. With the velocity fields obtained from the PIV measurements, we will be able to compare with the pivoting model proposed by Komar and Li (1986).

Motion Capture Techniques

SfM techniques hold great promise for resolving five degrees of freedom (the sixth degree, roll, cannot be readily determined) for submerged munitions as well providing data on bathymetry evolution with high time resolution. Much has been learned about optimizing feature pairing across images as well as thresholds for accuracy in reconstruction. Remaining challenges include identifying and tracking key regions in reconstructed meshes, as well as automating the cleaning processes of dense point clouds. Both obstacles need not be resolved before commencement of laboratory experiments. The second method, Motion Reconstruction from Feature Tracking, will be used in tandem as alternative technique and resolve munition roll.

Literature Cited

Friedrichs, C., (2013) "Simple Parameterized Models for Predicting Mobility, Burial and Re-Exposure of Underwater Munitions", MR-2224.

Kirchner, J. W., Dietrich, W. E., Iseya, F., & Ikeda, H. (1990). The variability of critical shear stress, friction angle, and grain protrusion in water-worked sediments. *Sedimentology*, ***37*** (4), 647-672.

Komar, P. D., and Li, Z. (1988). "Applications of grain-pivoting and sliding analyses to selective entrainment of gravel and to flow-competence evaluations," *Sedimentology*, **35**, 681-695

Komar, P. D., and Li, Z. (1986). Pivoting analyses of the selective entrainment of sediments by shape and size with application to gravel threshold. *Sedimentology*, ***33*** (3), 425-436.

Lowe, D. G. (2004). Distinctive image features from scale-invariant keypoints. *International journal of computer vision*, *60* (2), 91-110.

Raffel, M., Willert, C., Wereley, S., and Kompenhans, J. (1998). *Particle Image Velocimetry*. Berlin.

SERDP, (2010). "Munitions in the Underwater Environment: State of the Science and Knowledge Gaps", white paper. June

Zuniga Zamalloa, C., Hamed, A.M., Chamorro, L. P. (2014) "Feature tracking for measurement of translational and angular displacements of solid objects in fluid flows with application to saltation", *American Physical Society, Division of Fluid Dynamics 67th Annual Meeting*.

Appendix

Initiation of Motion Trials in Unidirectional Flows

Substrate	Flume (and slope)	Surrogate Munition Shape	Surrogate Munition Type	Manufacturer	Trials per Angle										Trial Subtotals
					0°	10°	20°	30°	40°	50°	60°	70°	80°	90°	
PVC	WHOI Flume (horiz. bed)	Cartridge	25-mm	NRL	*	1	1	1	1	1	1	1	1	1	10
				UIUC	0	0	0	1	0	0	1	0	0	1	3
			35-mm	NRL	-	-	-	1	-	-	1	-	-	1	10
				UIUC	*	1	3	1	1	1	1	3	1	1	14
			81-mm	NRL	-	-	-	-	-	-	-	-	-	-	10
				UIUC	*	1	1	1	1	1	1	1	1	1	10
		Warhead	25-mm	NRL	*	1	1	1	1	1	1	1	1	1	10
				UIUC	0	0	0	0	0	0	0	0	0	0	0
			35-mm	NRL	-	-	-	-	-	-	-	-	-	-	10
				UIUC	*	1	1	1	1	1	1	1	3	1	12
			81-mm (no fin)	NRL	-	-	-	-	-	-	-	-	-	-	10
				UIUC	0	3	4	3	5	4	3	3	4	5	34
Painted Pitted Steel	STF (Slope=0.4°)	Cartridge	25-mm	UIUC	*	2	0	4	0	0	4	0	0	0	11
			35-mm	UIUC	*	2	0	4	0	0	4	0	0	0	11
			81-mm	UIUC	*	2	0	4	0	0	3	0	0	0	10
		Warhead	25-mm	UIUC	*	0	0	*	0	0	*	0	0	*	4
			35-mm	UIUC	*	0	0	*	0	0	*	0	0	*	4
			81-mm (no fin)	UIUC	*	0	0	*	0	0	*	0	0	*	4
Painted Pitted Steel	STF (horiz. bed)	Cartridge	25-mm	UIUC	*	3	0	3	0	0	3	0	0	2	12
			35-mm	UIUC	*	3	0	4	2	0	2	0	0	3	15
			81-mm	UIUC	*	2	0	2	4	3	3	1	0	2	18
		Warhead	25-mm	UIUC	*	0	0	*	0	0	*	0	0	*	4
			35-mm	UIUC	*	0	0	*	0	0	*	0	0	*	4
			81-mm	UIUC	*	0	0	*	0	0	*	0	0	*	4
														Total Trials:	234

#	Data available: number represents trials performed
0	Trial not performed at this time
*	Motion could not be achieved on this surface under specified conditions
-	NRL Munitions no longer available at Ven Te Chow Lab

Table 5: Unidirectional flow experimental initiation of motion matrix illustrating the various trials for each experimental condition.